Journal of Nuclear Materials 408 (2011) 205–208

Contents lists available at ScienceDirect

Journal of Nuclear Materials

journal homepage: www.elsevier.com/locate/jnucmat

Letter to the Editor

A novel method for incorporating fission gas elements into solids

I.O. Usov [a,*], J. Won [a], D.J. Devlin [a], Y.-B. Jiang [b], J.A. Valdez [a], K.E. Sickafus [a]

[a] Los Alamos National Laboratory, Mailstop K763, Los Alamos, NM 87545, USA
[b] University of New Mexico, Albuquerque, NM, USA

ARTICLE INFO

Article history:
Received 29 July 2010
Accepted 3 November 2010

ABSTRACT

A novel method for the fabrication of test samples for fission gas behavior studies is described. We applied the technique of ion beam assisted deposition (IBAD) as a means to introduce Xe atoms into alumina (Al_2O_3) films. We then investigated the redistribution of Xe atoms and microstructural evolution induced by annealing. Transmission electron microscopy analysis revealed that the microstructure of our Al_2O_3–Xe IBAD films resemble characteristic microstructural features associated with fission gas accumulation in reactor-irradiated nuclear fuels.

1. Introduction

Basic information concerning quantitative descriptions of fission gas (Xe and Kr) behavior in nuclear fuel materials (both ceramic and metal forms) is lacking to an extent that it is impossible to predict their performance and verify modeling results. Xe is the major fission gas element, with concentrations reaching a few at.% in fuels at end-of-life. The combination of high concentrations of Xe and Xe insolubility leads to Xe bubble formation and attendant fuel matrix swelling, as well as to degradation of mechanical properties and thermal conductivity [1]. Release of Xe gas also reduces thermal conductivity in the fuel/clad gap and increases pressure in the fuel pin. This may result in the breach of the clad material and escape of radiotoxic products in the environment. Both effects are detrimental to fuel performance and therefore must be well-understood and controlled. Kr behavior is similar to Xe, except that its deleterious influence on fuel performance is less pronounced than Xe, because the concentration of Kr in fuel during service is about one order of magnitude less than Xe.

Up to now, information on fission gas release from nuclear fuel and fuel swelling is typically estimated using the FRAPCON code [2]. This code is based on a set of empirical equations and can be applied only to steady-state operating conditions. This is due to the fact that the fundamental physics underlying nucleation, growth, migration, resolution of fission gas bubbles and mechanisms of fission gas release are only partially understood. This limits the transferability of this code to new nuclear fuel materials, as well as to abnormal operating conditions. A major problem in formulating a theoretical model for fission gas behavior resides in the multitude of processes that take place simultaneously during fuel burning. These processes include: (1) variation of radial fuel temperature and stoichiometry; (2) microstructural changes (especially grain growth and texturing); (3) generation of point and extended defects; and (4) accumulation and migration of various fission products with different chemical states. All these processes greatly influence fission gas behavior. For instance, Nail [3] pointed out that the scatter of experimentally-measured Xe diffusion coefficients in UO_2 approaches seven orders of magnitude.[1]

In this paper, we demonstrate a novel new method for the uniform and controllable introduction of fission gas elements into solids. We introduce this method using the example of Xe doping alumina (Al_2O_3) thin films. Alumina is a prototypical ceramic oxide material. We chose alumina for these inaugural experiments because this material can be handled easily, with no need for special radioactive sample handling facilities. However, the method we describe herein is highly suitable for incorporating Xe into nuclear fuel materials such as U and UO_2.

2. Experimental details

Alumina (Al_2O_3) thin films were deposited on a carbon substrate at room temperature by electron beam evaporation. The alumina deposition rate was set to 1 nm/s. The pressure during the deposition was 1.6×10^{-4} Torr. During film growth, the film was simultaneously bombarded by low energy (800 eV) Xe^+ ions (ion beam current of 71 mA), incident at 45° with respect to the film

[1] These diffusion data were determined by two experimental methods [4]: (i) reactor irradiation of fissile material; and (ii) bombardment with Xe ions from an accelerator or an external fissionable source. It is very likely that the scatter in the diffusion coefficient values is related to fundamental drawbacks of both methods. The disadvantage of the ion bombardment method is the short range of energetic Xe ions, which leads to a pronounced influence of the sample surface. In experiments utilizing reactor irradiation, understanding fission gas behavior is limited, due to our inability to separate effects of fission gas introduction from various effects attendant to the fission process.

* Tel.: +1 505 667 3656; fax: +1 505 665 3164.
E-mail address: iusov@lanl.gov (I.O. Usov).

0022-3115/$ - see front matter © 2010 Elsevier B.V. All rights reserved.
doi:10.1016/j.jnucmat.2010.11.008

surface. This thin film growth method is referred to as ion beam assisted deposition (IBAD). IBAD is usually used as a technique to modify various physical properties of thin film coatings (density, texture, hardness, electrical resistivity, grain size etc.) [5–8]. It is important to note that a typical characteristic of IBAD films is that they are contaminated with gas atoms from the ion assist gun. Ar^+ is the most popular assist ion (primarily because of its low price) and it is always present in films fabricated using IBAD. In this study, we take advantage of the "impurity doping" feature of IBAD, by replacing Ar with Xe.

An as-deposited thin film Al_2O_3–Xe sample was cut in two pieces and one piece was annealed in vacuum ($\sim 10^{-6}$ Torr) at 800 °C for 1 h. This anneal was performed in order to investigate the effect of heat treatment on microstructural evolution and Xe redistribution. The as-deposited alumina film thickness and the depth distribution of incorporated Xe atoms, was measured using Rutherford backscattering spectrometry (RBS) using 2 MeV He^+ ions. RBS measurements indicated that the as-deposited alumina film is stoichiometric (Al_2O_3). The film thickness, estimated by RBS, was ~230 nm (assuming a density for Al_2O_3 of 3.96 g/cm^3). Microstructural analyses of Al_2O_3–Xe films before and after annealing were performed using scanning transmission electron microscopy (STEM), particularly using high-angle angular dark field (HAADF) imaging on JEOL 2010F instrument operating at 200 kV. For STEM analysis, the samples were prepared using standard methods: mechanical thinning and Ar ion milling.

3. Results and discussions

Fig. 1 shows the Xe concentration depth profile, estimated from RBS spectra by the SIMNRA code [9], in an Al_2O_3–Xe IBAD film before and after annealing. In the as-deposited sample, the Xe concentration is relatively uniform and corresponds to ~1 at.% in the near surface region. There is an increase in Xe concentration close to the interface with the carbon substrate. The concentration of Xe introduced by IBAD is controlled by varying the ratio of the deposition rate of the alumina film to the current density of the Xe ion assist beam. The lower (higher) this ratio, the higher (lower) the Xe concentration. RBS measurements also revealed that a small amount of Xe is incorporated in the carbon substrate during film growth, near the interface region with the alumina film. Interestingly, RBS found no evidence for Xe release from the alumina film after annealing. However, RBS did reveal evidence for some redistribution of the Xe during annealing. The fluctuation of Xe concentration near the carbon/Al_2O_3 interface in the as-deposited film (which we attribute to an instability of deposition conditions), became less pronounced following annealing.

RBS measurement on the annealed Al_2O_3–Xe film also revealed significant diffusion of Xe into the carbon substrate. The diffusion coefficient of Xe in carbon can be determined by fitting the experimentally-measured Xe depth profile with the analytical solution of Fick's equation for impurity diffusion from a constant source [10]:

$$C = C_0 \mathrm{erfc}\left(\frac{x}{2\sqrt{Dt}}\right), \quad (1)$$

where C_0 is the impurity concentration at the interface, x is the distance, D is the diffusion coefficient, and t is the annealing time. Based on our RBS measurements and using Eq. (1), we find that the diffusion coefficient for Xe in carbon at 800 °C is $\sim 2.5 \times 10^{-15}$ cm^2/s. To our knowledge this is the first experimental measurement of the Xe diffusion coefficient in carbon. Even though determination of this diffusion coefficient was not the focus of our study, it remains valuable information relevant to nuclear fuels. In particular, this information is useful to understand the behavior of TRISO fuel forms, wherein graphite (one of the allotropes of carbon) layers surround a UO_2 kernel in a spherical pellet fuel geometry [11].

Fig. 2 shows a cross-sectional HAADF/STEM image and an electron diffraction pattern (inset) obtained from the as-deposited Al_2O_3–Xe IBAD film. The electron diffraction pattern consists of a broad halo, which is indicative of an amorphous structure in the film. The HAADF STEM image, on the other hand, reveals a well-arranged set of bright and dark bands. Moreover, these bands are parallel to the carbon/Al_2O_3 interface. The HAADF image contrast is proportional to the atomic number (Z) of the material; thus HAADF images are typically referred to as "Z-contrast" images. This said, the regions of bright and dark contrast in Fig. 2 are attributable to the presence of high-Z and low-Z elements, respectively. In particular, the dark bands in Fig. 2 are presumably representative of layers containing primarily Al_2O_3, while the light bands

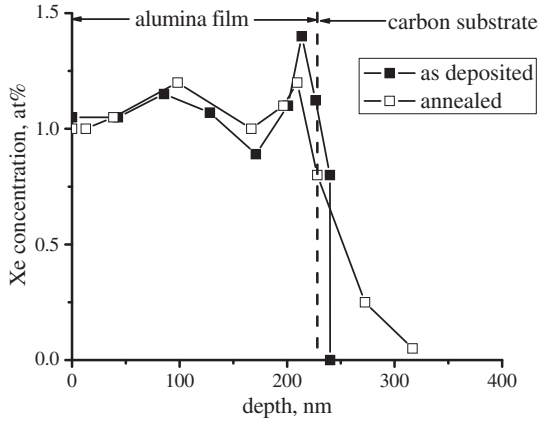

Fig. 1. Concentration depth profiles of Xe in as-deposited and post-annealed (in vacuum at 800 °C for 1 h) Al_2O_3–Xe IBAD films deposited on a carbon substrate. Lines are shown merely to guide the eye.

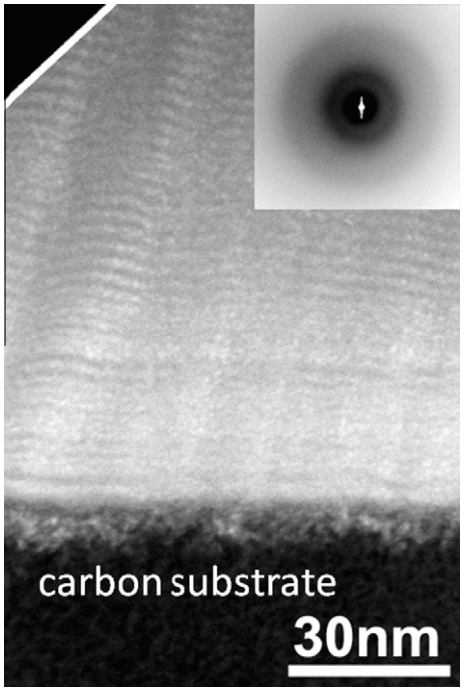

Fig. 2. Cross-sectional HAADF/STEM image and electron diffraction pattern (inset), obtained from an as-deposited Al_2O_3–Xe IBAD film.

are likely alumina with significant Xe-enrichment. Both light and dark bands have similar widths of ~1.5 nm. It should be noted that the depth resolution of the RBS technique (results shown in Fig. 1) is ~20 nm (at the sample surface). Consequently, we did not resolve by RBS (Fig. 1) the fine-scale compositional modulation revealed by STEM in Fig. 2. At present, we have not established whether or not the light-contrast bands consist of uniformly-dispersed Xe atoms or rather are chains of small Xe bubbles. Nevertheless, it is interesting to compare our as-deposited Al_2O_3–Xe IBAD thin film microstructure with other actual irradiated fuel microstructures. Indeed, Van den Berghe et al. [12] in a study of a dispersion metal nuclear fuel (U–Mo), showed an almost identical structure of alternating dark/light bands of contrast due to fission gas accumulation (see Fig. 4a in Ref. [12]). The similarities between the microstructure observed in Fig. 2 (this report) and in Ref. [10] are striking, considering that the sample histories are completely different. Van den Berghe et al. [12] attributed their banded microstructure to the formation of regularly-spaced bubbles or voids within the U(Mo) matrix. In a more recent study of dispersion metal nuclear fuel microstructure evolution due to fission gas accumulation, it was suggested that the formation of a fission gas bubble superlattice is an effective mechanism for the incorporation of insoluble Xe and Kr atoms [13]. However, the nature of this effect is not understood. The only reported ordering of fission gas bubbles in ceramic nuclear fuel relates to the observation that fission gas bubbles in UO_2 tend to be arranged in straight lines. The most plausible mechanism for producing these lines is spontaneous bubble nucleation along fission fragment tracks [14]. The segregation of Xe into alternating layers that we observe in our Al_2O_3–Xe samples cannot arise from this mechanism, because the energy of our Xe^+ assist ions is too low compared to the high (tens of MeV) fission fragment energies responsible for track formation.

Another explanation for the banded contrast in Fig. 2 is possible modification of the microstructure induced during STEM sample preparation (this consists of mechanical thinning followed by Ar^+ ion milling). Examples of sample preparation artifacts might include: (1) areas of diminished sample thickness; or alternatively, (2) a partial Xe gas release that leaves behind void-like regions. Both of these artifacts could cause an appearance of regions with darker contrast. However, why these regions are parallel to the substrate/film interface and are so well-arranged, is not clear to us at present.

One additional notable feature in Fig. 2 is the *Z*-contrast evidence that Xe penetrates into the carbon substrate, to a depth ~10 nm below the carbon/Al_2O_3 interface. This observation corroborates the RBS evidence for Xe penetration into the carbon substrate shown in Fig. 1 (for as-deposited sample).

Fig. 3 shows a micrograph of the microstructure of the post-annealed (800 °C/h) Al_2O_3–Xe IBAD film. This micrograph was obtained using HAADF/STEM imaging. After annealing, the Al_2O_3–Xe IBAD film was found to be a mixture of crystalline and amorphous phases (diffraction evidence for partial crystallinity is not shown in Fig. 3). In addition, the thin film microstructure changed profoundly upon annealing. The light and dark bands disappeared and well-defined cavities (regions of dark contrast labeled with double arrows) formed throughout the film thickness. These cavities presumably contained Xe prior to STEM sample preparation, but escaped during the sample preparation process. The measured dimensions of these cavities ranged from 2 to 9 nm. Also in Fig. 3, there are small bright spots, 1–2 nm in diameter, which we believe are Xe bubbles. Interestingly, the sizes of the Xe bubbles in our post-annealed Al_2O_3–Xe IBAD film are similar to those formed in UO_2 irradiated with thermal neutrons (1.5–3 nm) [14].

Our observation of the formation of Xe bubbles induced by annealing suggests that Xe (dispersed atomically or in the form of small bubbles, with dimensions less than 1.5 nm), has substantial mobility in amorphous alumina. The absence of Xe release from the alumina film established by RBS suggests that trapping of Xe in growing, immobile bubbles, occurs in the early stages of annealing.

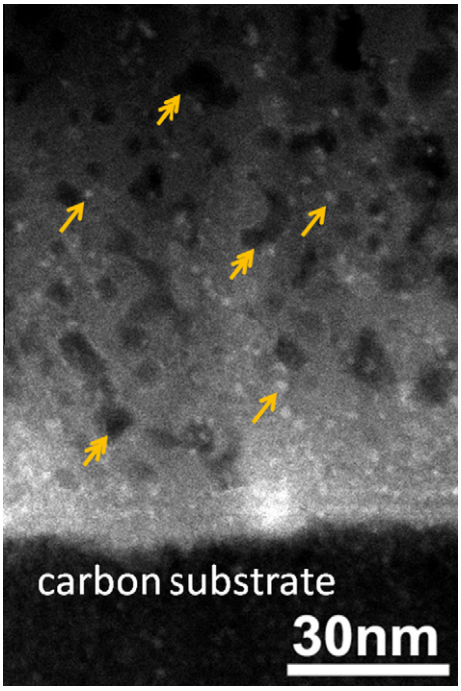

Fig. 3. Cross-sectional HAADF/STEM image obtained from a post-annealed alumina Al_2O_3–Xe IBAD film (annealed in vacuum at 800 °C for 1 h). Single arrows indicate Xe bubbles. Double arrows indicate cavities or voids.

4. Summary

Our understanding of fission gas behavior in nuclear fuel materials is limited, due to the multitude of atomistic and microstructural processes that occur in a fuel during service. In this paper, we demonstrated a novel method to introduce Xe (a typical fission gas element) into alumina (Al_2O_3) thin films (a prototypical ceramic oxide material), using the IBAD method. We found that the size and spatial distributions of Xe bubbles in our post-annealed, Al_2O_3–Xe IBAD films, are similar to the fission gas bubbles observed in UO_2 irradiated with thermal neutrons. We also demonstrated that the microstructure of our as-deposited Al_2O_3–Xe IBAD films have features in common with other irradiated nuclear fuel materials (namely dispersion metal fuels). We note that other gaseous elements such as Kr and He can be introduced into all sorts of solids (metals, oxides, carbides and nitrides) by IBAD. In our deposition set-up, deposition rates can be as high as 10 μm/h. This makes it possible to fabricate bulk-like samples (a few 100 μm thick or more), uniformly doped with fission gas elements. The value of such samples is that fission gas introduction is separated from the various effects attendant to the fission process. Our future goal is to examine bubble/cavity evolution in real, "fuel-like" materials doped with fission gas elements (e.g., U and UO_2).

A most important feature of the IBAD process for incorporating gaseous species into solid matrices is the possibility to introduce fairly large, yet homogeneous concentrations of gas (several at.%) into a solid, over thicknesses as large as several hundred microns. Currently, reactor irradiation of fissile material is the only method

to introduce a (nearly) uniform concentration of fission gas atoms. But following reactor irradiation, the fuel has changed composition significantly and is highly radioactive. Our new technique offers the opportunity to develop a radiation-free, composition-controlled, systematic approach to elucidating the underlying physics of gas behavior in nuclear materials.

Acknowledgements

This work was supported by the US Department of Energy Office of Basic Energy Sciences, Division of Materials Sciences and Engineering and by a Los Alamos National Laboratory, Laboratory Directed Research and Development (LDRD) Grant. RBS analysis was performed at the Ion Beam Materials Laboratory (IBML) at Los Alamos National Laboratory and HADDF/STEM observation was performed at the University of New Mexico (UNM). The authors would like to thank J. Tesmer, R. Greco and Y. Wang from the IBML facility, and Ying-Bing Jiang from UNM for their technical assistance.

References

[1] D.R. Olander, Fundamental aspects of nuclear reactor fuel elements, Technical Information Center, Office of Public Affairs, Energy Research and Development Administration, Springfield, Virginia, 1976.
[2] http://www.pnl.gov/frapcon3/.
[3] M.C. Nail, Diffusion controlled and burst release of gaseous and volatile fission products from UO_2 and ThO_2, in: R.P. Agarwala (Ed.), Diffusion processes in nuclear materials, Elsevier Science Publishers, North-Holland, 1992.
[4] H. Matzke, J. Nucl. Mater. 53 (1980) 219.
[5] R.A. Roy, J.J. Cuomo, D.S. Yee, J. Vac. Sci. Technol. A 6 (1988) 1621.
[6] P.J. Martin, R.P. Netterfield, W.G. Sainty, J. Appl. Phys. 55 (1984) 235.
[7] P. Ziemann, E. Kay, J. Vac. Sci. Technol. A 1 (1983) 512.
[8] P.N. Arendt, S.R. Foltyn, MRS Bull. 29 (2004) 543.
[9] M. Mayer, SIMNRA User's Guide, Report IPP 9/113, Max-Planck-Institut fur Plasmaphysik, Garching, Germany, 1997.
[10] D. Shaw, Atomic Diffusion in Semiconductors, Plenum press, London, UK, 1973.
[11] J.J. Powers, B.D. Wirth, J. Nucl. Mater. 405 (2010) 74.
[12] S. Van den Berghe, W. Van Renterghem, A. Leenaers, J. Nucl. Mater. 375 (2008) 340.
[13] J. Gan, D.D. Keiser Jr., D.M. Wachs, A.B. Robinson, B.D. Miller, T.R. Allen, J. Nucl. Mater. 396 (2010) 234.
[14] J.A. Turnbull, J. Nucl. Mater. 38 (1971) 202.